

## Supplementary information

# The effect of the buffer solution on the adsorption and stability of horse heart myoglobin in commercial mesoporous titanium dioxide: a matter of the right choice.

Stefano Loreto, Bert Cuypers, Jacotte Brokken, Sabine Van Doorslaer, Karolien De Wael and Vera Meynen\*

## Content

Buffer effect on protein stability in solution	2
Interaction between the different buffers and the mesoporous TiO <sub>2</sub>	2
Buffer effect on the adsorption of horse heart myoglobin	3
Structural stability of horse heart myoglobin upon adsorption in different buffers	4

## Buffer effect on protein stability in solution

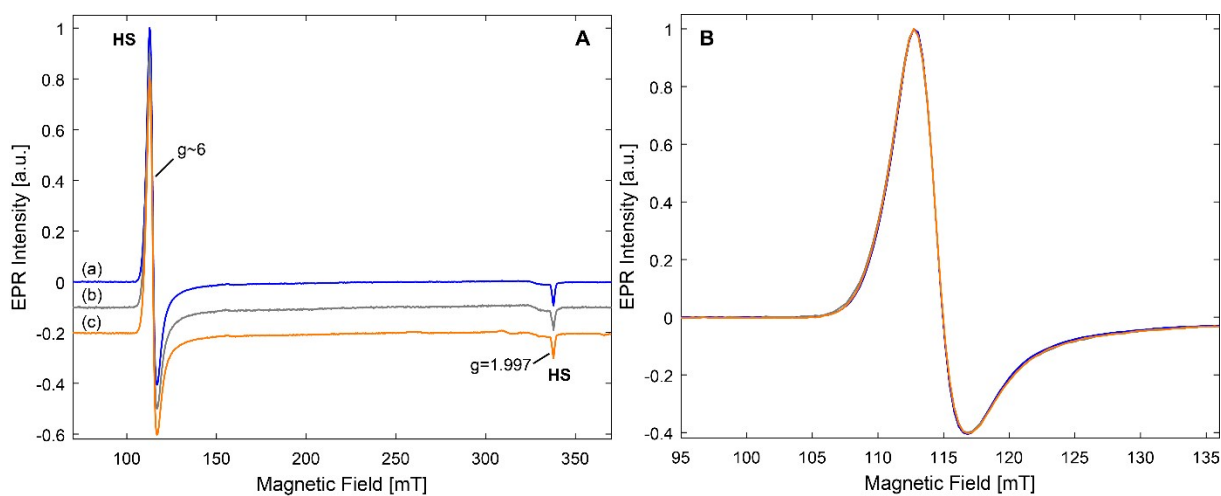


Fig. S.I. 1. CW-EPR spectra of a frozen solution of 0.5 mM hhMb in HEPES buffer (blue, (a)), PBS buffer (grey, (b)) and Tris buffer (orange, (c)). **A** shows the full spectrum and **B** is a detailed view in the range 95-136 mT. The feature stemming from the high-spin (HS) iron heme center is indicated in the spectra in **A**, as well as the contribution of a non-heme iron, which is indicated with an asterisk. All spectra are rescaled to the same microwave frequency and normalized to equal intensity for facile comparison.

## Interaction between the different buffers and the mesoporous TiO<sub>2</sub>

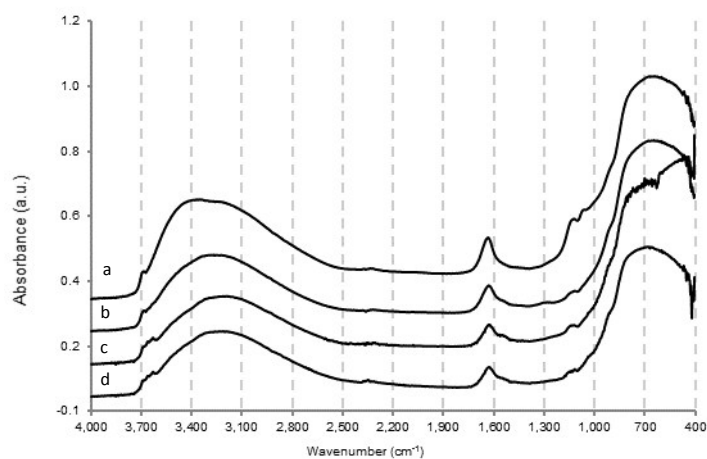


Figure S.I.2. IR spectra (offset 0.01) of Mil-PBS (a), Mil-Tris (b), Mil-H<sub>2</sub>O (c) and Mil-HEPES (d).

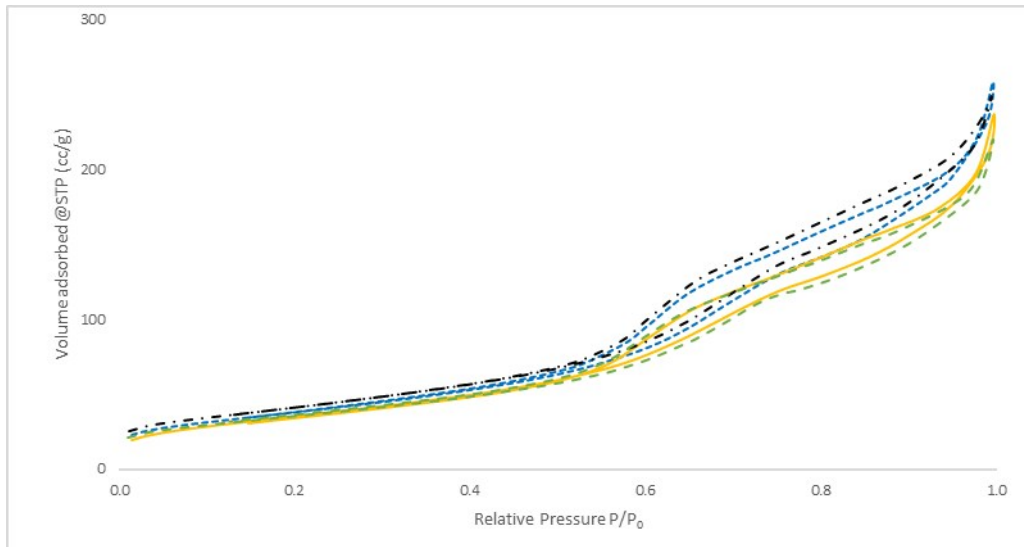


Fig. S.I. 3.  $N_2$  sorption isotherms of Mil- $H_2O$  (black, dashed dotted line), Mil-HEPES (blue, dotted line), Mil-Tris (yellow, solid line) and Mil-PBS (green, dashed line) after degassing 16h at 25°C.

### Buffer effect on the adsorption of horse hearth myoglobin

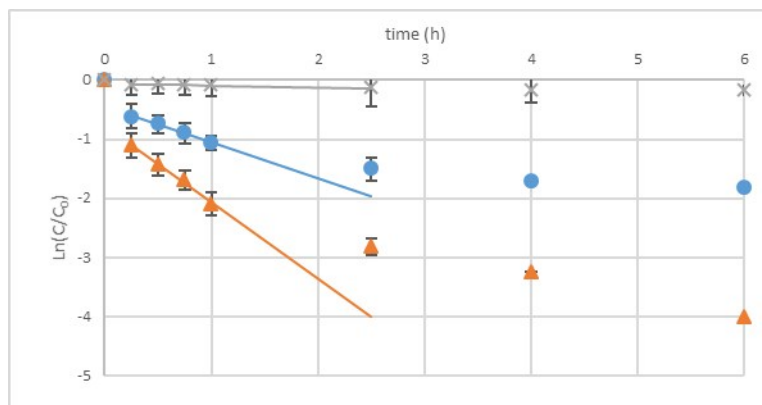


Figure S.I.4. Time evolution of  $\ln(C/C_0)$  in HEPES (orange,  $\Delta$ ), Tris (blue,  $\bullet$ ) and PBS (gray,  $\times$ ) solution during the first 6 hours of shaking. The straight lines obtained from measurements after 1h of shaking (solid lines) were used for the evaluation of the kinetic constant  $k_s$ . The error bars are calculated on a set of three measurements.

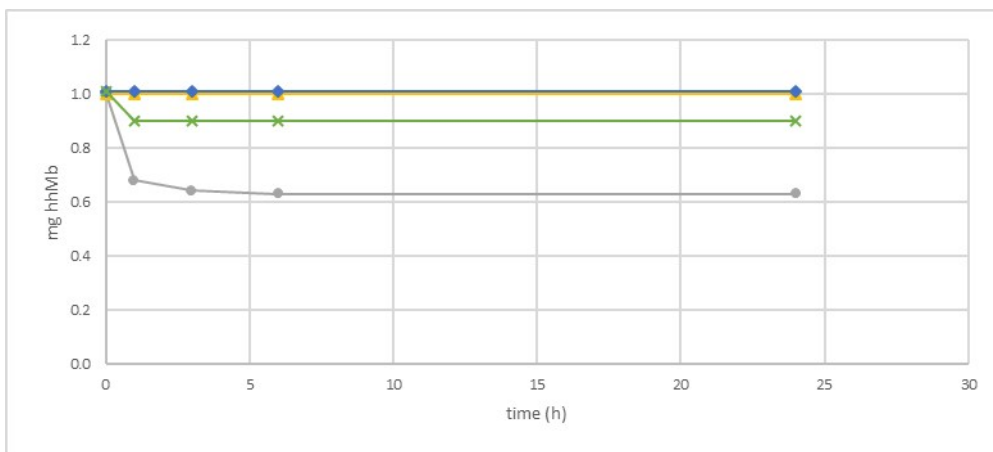


Fig. S.I. 5. Leaching tests performed by first incorporating hhMb-Mil-HEPES and Tris (subsequent washing and drying) and then dissolving the hhMb-Mil-HEPES in a new HEPES (yellow line,  $\Delta$ ), Tris (blue line,  $\diamond$ ) and PBS (gray line,  $\bullet$ ) solution and the hhMb-Mil-Tris in PBS (green line,  $\square$ ). The amount of leached proteins was estimated by UV-vis spectroscopy.

### Structural stability of horse heart myoglobin upon adsorption in different buffers

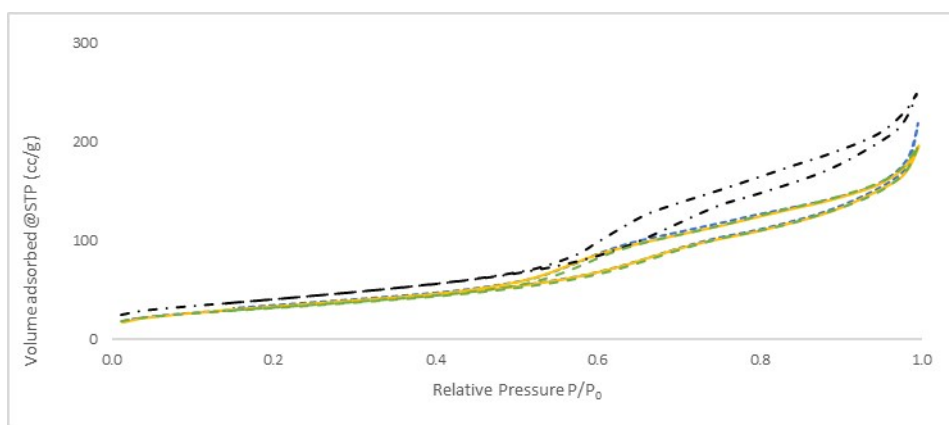


Fig. S.I. 6.  $N_2$ -sorption isotherms of calcined Millennium (black, dashed dotted line), hhMb-Mil-HEPES (blue, dotted line), hhMb-Mil-Tris (yellow, solid line) and hhMb-Mil-PBS (green, dashed line) after degassing for 16h at 25°C.

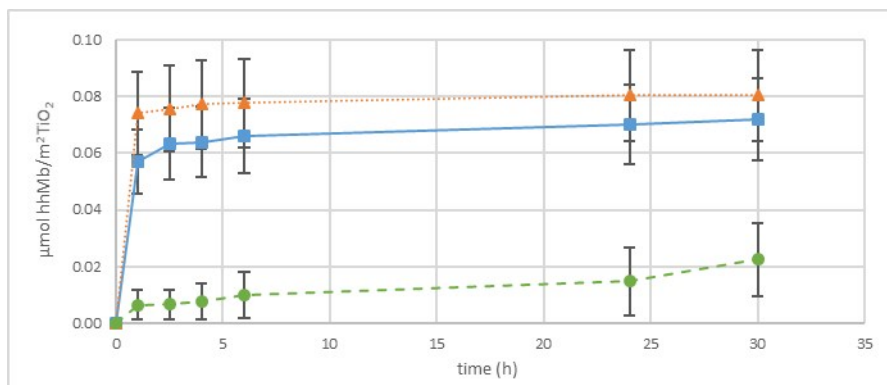


Fig. S.I. 7. Adsorption of hhMb on the non-porous P25 in HEPES (dotted line), Tris (solid line) and PBS (dashed line) solution. The concentration of the buffer is 10 mM. The results are expressed as amount of proteins (in  $\mu\text{mol}$ ) per  $\text{m}^2$  of  $\text{TiO}_2$  versus shaking time. Error bars are calculated on a set of three measurements.

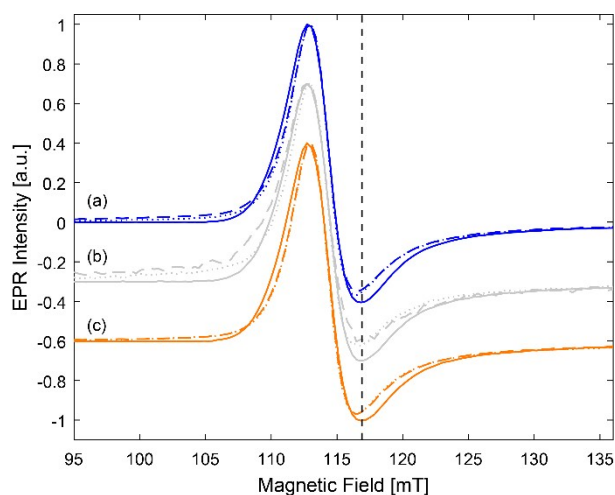


Fig. S.I. 8. Low-field part of the CW-EPR spectra of frozen solution of hhMb (solid line) and hhMb incorporated in Millennium before (dashed line) and after (dotted line) drying of the final powder. The incorporation was done in HEPES buffer (blue, (a)), PBS buffer (grey, (b)) and Tris buffer (orange, (c)). All spectra are rescaled to the same microwave frequency and normalized to equal intensity for facile comparison.

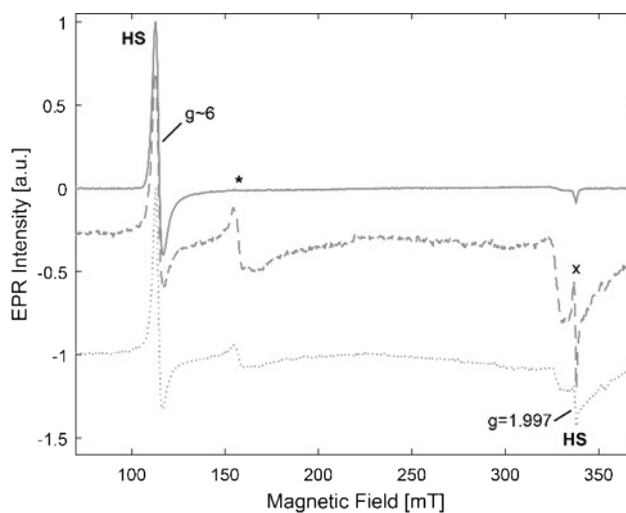


Fig. S.I. 9. CW-EPR spectra of frozen solution of hhMb (solid line) and hhMb incorporated in PBS buffer in Millennium before (dashed line) and after (dotted line) drying of the final powder. The contribution of high-spin feature (HS), a small radical (x) and a non-heme iron are indicated. All spectra are rescaled to the same microwave frequency and normalized to equal intensity for facile comparison.

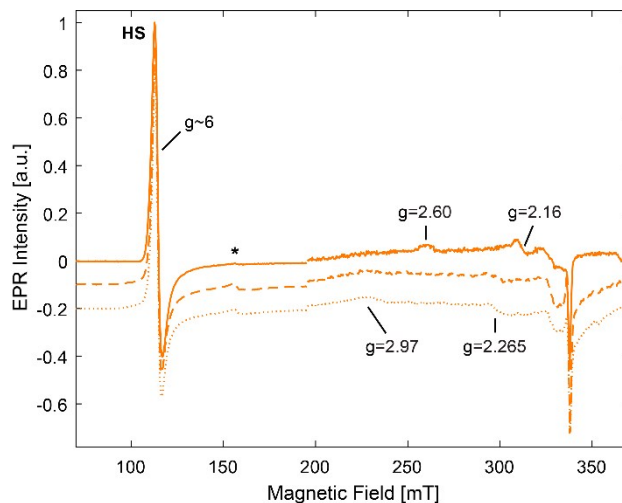


Fig. S.I. 10. CW-EPR spectra of frozen solution of hhMb (solid line) and hhMb-Mil-Tris before (dashed line) and after (dotted line) drying of the final powder. The contribution of a high-spin feature (HS) and a non-heme iron are indicated. All spectra are rescaled to the same microwave and normalized to equal intensity for facile comparison. The LS form with  $g_x=2.60$  and  $g_y=2.16$ , present in hhMb, can be ascribed to hydroxide-coordinated hhMb, while a weak LS form with  $g_x=2.97$  and  $g_y=2.265$  is visible in the hhMb-Mil-Tris spectra.

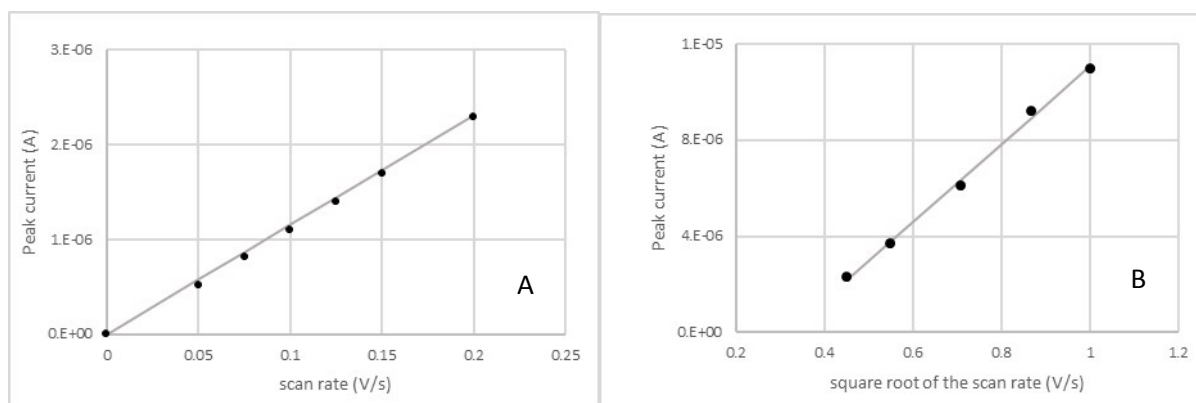


Fig. S.I. 11. Dependence of the reduction peak current from the scan rate (A) and the square root of the scan rate (B) for hhMb-Mil-HEPES at pH 7 in PBS 0.1M.

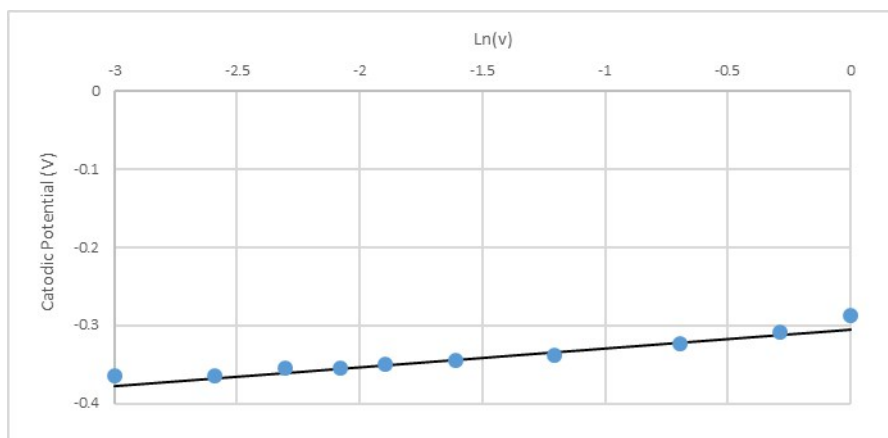


Figure S.I.12. Influence of the scan rate (logarithmic scale) on the cathodic peak potential of hhMb-Mil-HEPES at pH 7 in PBS buffer in PBS 0.1M.